analytical chemistry

Article

pubs.acs.org/ac

Model-Based Classification for Digital PCR: Your Umbrella for Rain

Bart K. M. Jacobs,[*,†] Els Goetghebeur,[†] Jo Vandesompele,[‡,¶,§] Ariane De Ganck,[¶] Nele Nijs,[¶] Anneleen Beckers,[¶] Nina Papazova,[∥] Nancy H. Roosens,[∥] and Lieven Clement[*,†,§]

[†]Department of Applied Mathematics, Computer Science and Statistics, Ghent University, Ghent, Belgium

[‡]Center for Medical Genetics Ghent (CMGG), Ghent University, Ghent, Belgium

[¶]Biogazelle, Zwijnaarde, Belgium

[§]Bioinformatics Institute Ghent From Nucleotides to Networks (Big N2N), Ghent University, Ghent, Belgium

[∥]Scientific Institute of Public Health (WIV-ISP), Brussels, Belgium

Supporting Information

ABSTRACT: Standard data analysis pipelines for digital PCR estimate the concentration of a target nucleic acid by digitizing the end-point fluorescence of the parallel micro-PCR reactions, using an automated hard threshold. While it is known that misclassification has a major impact on the concentration estimate and substantially reduces accuracy, the uncertainty of this classification is typically ignored. We introduce a model-based clustering method to estimate the probability that the target is present (absent) in a partition conditional on its observed fluorescence and the distributional shape in no-template control samples. This methodology acknowledges the inherent uncertainty of the classification and provides a natural measure of precision, both at individual partition level and at the level of the global concentration. We illustrate our method on genetically modified organism, inhibition, dynamic range, and mutation detection experiments. We show that our method provides concentration estimates of similar accuracy or better than the current standard, along with a more realistic measure of precision. The individual partition probabilities and diagnostic density plots further allow for some quality control. An R implementation of our method, called Umbrella, is available, providing a more objective and automated data analysis procedure for absolute dPCR quantification.

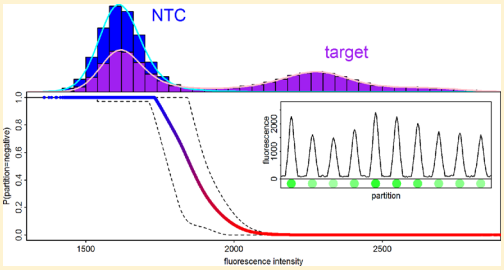

Recently, digital PCR has become a mainstream technology for detecting and quantifying nucleic acids (NAs), e.g., in genetically modified organism (GMO) analysis,[1,2] viral diagnostics,[3,4] copy number variation,[5] and mutant detection, among others. The technology uses chips or emulsion droplets to generate hundreds to millions of tiny partitions in which parallel micro-PCR reactions are performed on diluted template material from a sample. The end-point fluorescence is used to classify each partition as positive if an amplified target is detected, or negative if no amplification is found. Finally, the concentration of the target template can be estimated based on the number of positive and negative partitions, the partition volume, and the assumption that the number of copies in a partition follows a Poisson distribution. Often, several dyes are combined for assessing multiple NA targets simultaneously.

We recently showed that partition misclassification can have a major impact on the accuracy of dPCR.[6] This is illustrated in Figure 1, which presents fluorescence intensities from different experiments on GMOs. Classification based on an automated threshold, provided by QuantaSoft companion software from the Bio-Rad QX100 Digital Droplet PCR system, is questionable at best. The center of the positive and negative cluster can be estimated easily in both experiments, but the classification of partitions that are between those centers is difficult, especially in the right panel. Partitions that do not clearly belong to the positive or negative cluster are often called rain. However, manually tuning the threshold as an alternative for the undisclosed QuantaSoft procedure may introduce confirmation and researcher's bias. In Figure 1B, changing the threshold to include most rain in one of the clusters could lead to as few as 7000 and as many as 9500 positive partitions and a relative difference of 50% in the concentration estimates.

Hence, better classification methods are a priority to further improve the accuracy in dPCR experiments. New data-driven methods to calculate an improved hard threshold were proposed,[7,8] while others simply remove the problematic partitions called "rain".[4,9] Since the proportion of positive partitions in the rain can differ from the proportion of positive partitions in the sample, selective removal of rain will often introduce bias. Moreover, current dPCR data analysis workflows typically ignore the uncertainty of hard thresholding fluorescence signals into positive and negative partitions, consequently communicating concentration estimates with unrealistic precision and accuracy.

Received: October 27, 2016
Accepted: March 27, 2017
Published: March 28, 2017

DOI: 10.1021/acs.analchem.6b04208
Anal. Chem. 2017, 89, 4461−4467

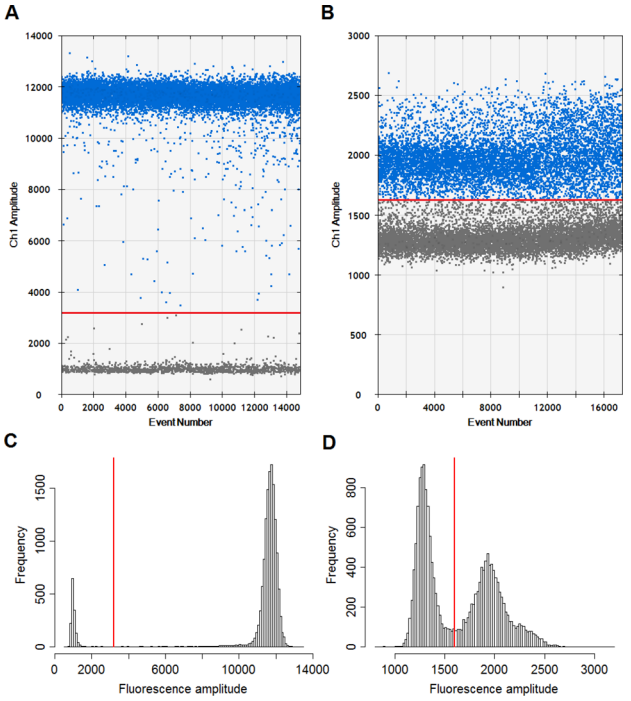

Figure 1. Fluorescence densities of different experiments. In panels (A) and (C), the fluorescence intensities are well-separated between positive and negative partitions. In panels (B) and (D), the right tail of the null density (in gray) overlaps with the left tail of the positive partitions (in blue), and considerable classification uncertainty can be expected for many partitions. The red line denotes QuantaSoft's automated threshold for classification.

However, accurate and realistic measures of precision are of vital importance[10] and may be scrutinized extensively in fields such as disease diagnostics[11] and genetically modified organism (GMO) testing.[12] Validated quantification tools for GMOs in food, for instance, are mandatory for the labeling of products containing GM ingredients implied by the European Union Regulations.[13,14]

We develop a model-based clustering method to classify partitions, which assumes that observed intensities are drawn from a mixture density with two components: one for the partitions containing the target (positive) and the other for partitions void of the target (negative). Using Bayes' rule, our method provides estimates of the probability that a partition belongs to a specific cluster conditional on its observed fluorescence, acknowledging the inherent classification uncertainty.[15] This probabilistic approach provides (i) more informed and objective global concentration estimates, and (ii) more realistic measures of precision that account for the classification uncertainty.

Moreover, the individual partition probabilities are very useful for quality control and in experiments that focus on the detection of a target NA based on the mere presence of positive partitions, rather than their number.

MATERIALS AND METHODS

We first introduce some terminology. A "partition" is an amount of reaction mix submitted in a single reaction, typically at the nanoliter or picoliter level, within a single droplet, chamber, or microwell. A "partition set" refers to the set of all partitions in one technical replicate of an experiment (typically a single well in droplet-based systems or an array in chamber-based systems). Technical replicates are multiple partition sets from the same biological sample run under the same conditions, while biological repeats are multiple partition sets from distinct biological samples with the same properties. A "run" or "experiment" is the joint name for a group of partition sets that aim for the same target.

Mixture Model. We assume that fluorescence intensities x observed in partitions of a target partition set A follow a mixture density $f_A(x)$:

$$f_A(x) = p_{0,A} f_{0,A}(x) + (1 - p_{0,A}) f_{1,A}(x)$$

with $f_{0,A}(x)$ and $f_{1,A}(x)$ being the densities of the partitions without and with target copy, respectively, and $p_{0,A}$ and $(1 - p_{0,A})$ is the proportion of negative and positive partitions. This is illustrated in Figure S-1 in the Supporting Information for

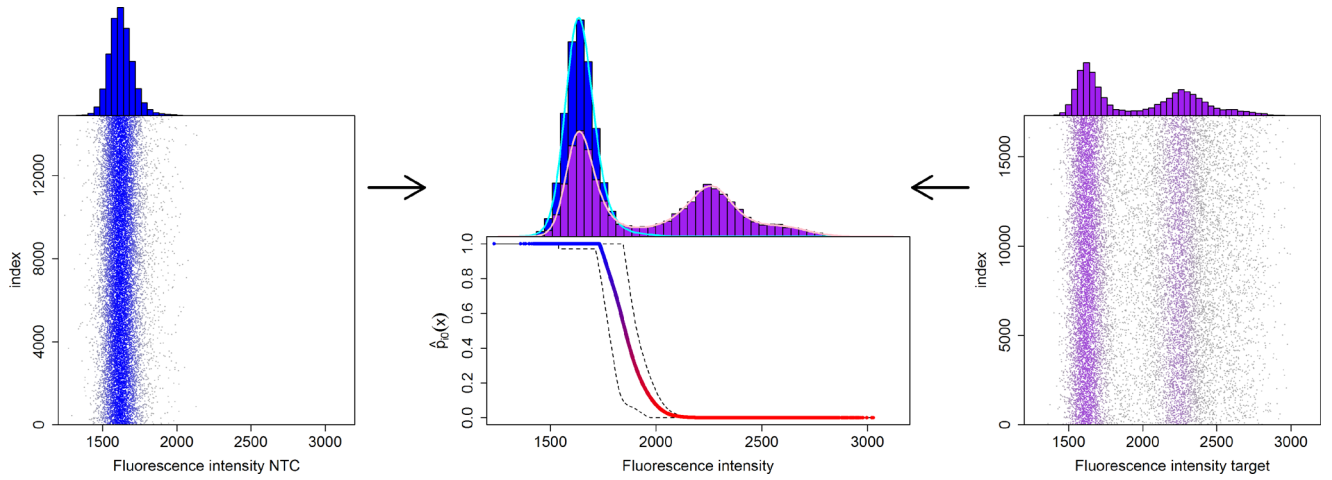

Figure 2. Fitting the mixture model using target and NTC partition sets. A generalized additive Poisson model is jointly fitted to aligned NTC (left panel) and target (right panel) fluorescence intensity histogram counts. Corresponding nonparametric density estimates for the NTC $\hat{f}_0$ (cyan) and target well $\hat{f}_A$ (pink) are displayed in the top-middle panel. The bottom-middle panel depicts posterior probabilities that a partition is void of the target. When multiple NTCs are available, confidence intervals can be provided reflecting the classification uncertainty due to between NTC variability (dashed lines).

DOI: 10.1021/acs.analchem.6b04208
Anal. Chem. 2017, 89, 4461−4467

different settings of rain. The parameter $p_{0,A}$ is used to convert the dPCR signal into a concentration estimate relying on the Poisson assumption. Note that state-of-the-art dPCR methods estimate $p_{0,A}$ as the proportion of negative partitions upon hard thresholding.

In many applications, model-based clustering builds on mixtures of normal densities $f_{0,A}(x)$ and $f_{1,A}(x)$ to facilitate identifiability and yield stable and precise estimates. However, early evidence suggests that dPCR partition densities cannot be easily parametrized. The theoretical distribution of fluorescence intensities was shown to be non-normal[8,16] and is influenced by technical factors such as partition volume[17,18] and "cross-talk" with the dyes of other channels.[19] This is confirmed in Figure 1, where heavy tails to the right and left are prominent for the negative and positive clusters, respectively, even in the example with limited rain (Figure 1C).

In the absence of obvious alternative parametric models for the component densities, we resort to nonparametric density estimation. We start by estimating marginal density $f_A(x)$ in the target partition set A. The associated nonparametric density estimation can be recasted into a Poisson regression problem.[20] Since $f_A(x)$ is one marginal density, the component densities are no longer identifiable from a single partition set. However, the marginal distribution of no-template control samples (NTCs) from the same experiment can be interpreted as a realization of the overall null density of background fluorescence and we estimate the negative component $f_{0,A}(x)$ by borrowing the shape (modulo standardization) of the NTC distribution.

Parameter Estimation. The rationale of our method is introduced in Figure 2 and Figure S-2 in the Supporting Information.

(1) The modes of the null component of the fluorescence densities of the target $f_A(x)$ and the NTC reference $f_0(x)$ are aligned.

(2) The aligned fluorescence intensities of the NTC and target are discretized using histograms with the same bins.

(3) The bin counts of the NTC reference and target partition set A are jointly modeled within a single Poisson regression model, as described in the Supporting Information. This model provides estimates $\hat{p}_{0,A}$, $\hat{f}_0(x)$, and $\hat{f}_A(x)$.

(4) The concentration of interest is derived from $\hat{p}_{0,A}$, using the Poisson assumption, i.e., the average number of template molecules per partition $\hat{\lambda}_A = -\ln(\hat{p}_{0,A})$ and the estimated concentration of the original sample $\hat{c}_A = \hat{\lambda}_A D/V_A$, with V being the volume of a partition, and D the dilution factor.[8] This is what we will call the main Umbrella estimator.

Model-Based Clustering. The mixture model also provides posterior probabilities $p_{i,0,A}$ that partition i of set A with fluorescence intensity x_i is void of the target sequence:

$$\hat{p}_{i,0,A} = \hat{p}_{0,A}\left(\frac{\hat{f}_{0,A}(x_i)}{\hat{f}_A(x_i)}\right)$$

However, this estimator is not bound to decrease monotonically with increasing fluorescence intensities. Therefore, we propose an additional bounded antitonic regression step on the estimated partition probabilities to enforce monotonicity. Final probabilities $\hat{p}_{i,0,A}$ are useful in various applications.

(1) As an Alternative Estimator for $p_{0,A}$ (e.g., in Detection Experiments). In addition to the aforementioned results, our procedure reports the number of partitions that have a probability $\hat{p}_{i,0,A}$ >80% (negative partitions with a probability of, at most, 20% to be a false negative), $\hat{p}_{i,0,A}$ < 5% (positive partitions with a probability of, at most, 5% to be a false positive), and 5% ≤ $\hat{p}_{i,0,A}$ ≤ 80% (rain). One minus the ratio of positive partitions ($\hat{p}_{i,0,A}$ < 5%) over the total is reported as an alternative estimator for $p_{0,A}$. This is what we will call Umbrella's threshold estimator. In detection experiments where the absolute number of positive partitions is often very low, Umbrella may not be precise and methods that classify individual partitions are more useful to address the detection problem.

Note that, generally,

$$\hat{p}_{0,A} \approx \sum_{i=1}^{n_A} \frac{\hat{p}_{i,0,A}}{n_A}$$

Hard thresholding is a special case where K partitions are classified as negative and have probability $p_{i,0,A} = 1$ and the remaining partitions are considered to be positive with probability $p_{i,0,A} = 0$.

(2) For Quality Control. Heavy tails, volume effects and inhibition can be identified by studying the relative decrease of $\hat{p}_{i,0,A}$ in the right tail of $f_{0,A}$. Both the absolute number of partitions in the rain as well as the precision of individual partition probabilities in the rain may be informative.

No-Template Controls. If multiple no-template controls (NTCs) are available, our procedure will be repeated for every partition set and every NTC within the same experiment. Results from multiple NTCs for the same target will be used to improve the concentration estimate and to quantify its associated precision.

No-template controls (NTCs) play an important role in qPCR and are also very useful in dPCR applications.[21] Depending on primer and probe sequence and concentration, they can look remarkably different between and even within experiments (see Figure S-4 in the Supporting Information). Ideally, NTCs mimic the real sample as closely as possible, without containing the target sequence, i.e., they should include all reaction components and preferably would undergo the same sample prep as real samples. In addition, it is good practice to provide multiple NTCs to capture their variability and to account for the corresponding uncertainty, both at individual partition and overall concentration level. Our method is able to propagate this information into the corresponding confidence intervals (see the Supporting Information (Section 6) for more details).

Multichannel Extension. Umbrella, which is similar to current state-of-the-art methods, is developed for single-channel data but can be trivially extended to multichannel data by adopting it repeatedly on the fluorescence intensities of multiple channels. Note that overlapping color spectra of the dyes, so-called "cross-talk"[19] and calibration issues can lead to rotational problems in the true multivariate null distribution and to differences for partitions that have a different status (pos/neg) in at least one other channel. Current state-of-the-art methods, such as hard thresholding, largely ignore these features.

We have developed an automated procedure for two-channel data that orthogonalizes rotated data and corrects for possible cross-talk. We are currently extending this to higher dimensions. Details can be found in the Supporting Information (Section 7).

DOI: 10.1021/acs.analchem.6b04208
Anal. Chem. 2017, 89, 4461−4467

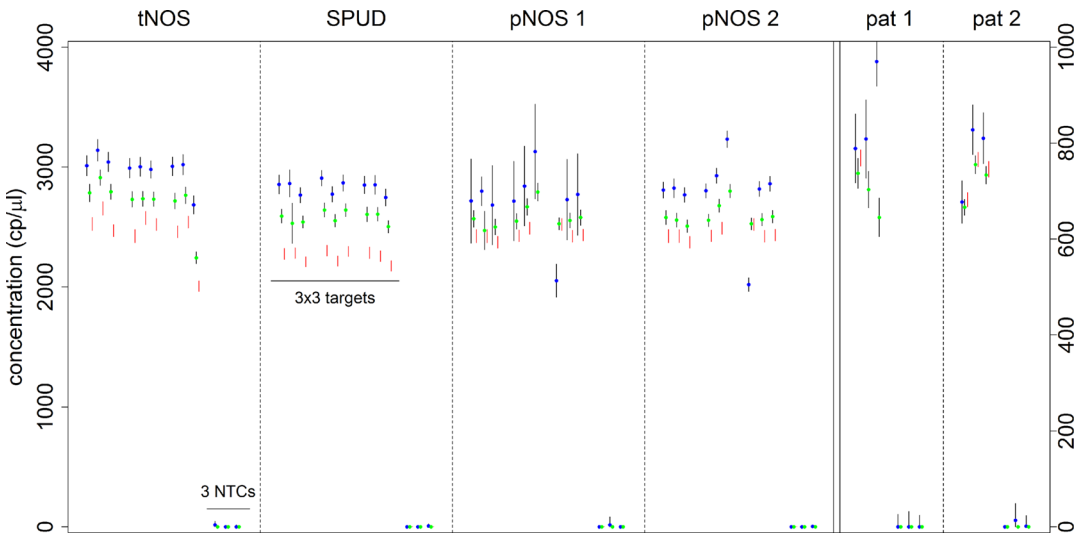

Figure 3. Concentration estimates for GMO data. The concentration estimates with their respective confidence intervals (CIs) are displayed for four different targets. For each experiment except pat 1 and pat 2, a dilution was aliquoted in three vials that were each analyzed with three technical replicates. The technical replicates for each vial are plotted adjacently. The last three results for every target are the NTCs. The black CIs with blue concentration estimates (CEs) were obtained with the main Umbrella estimator, the black CIs with the green CEs were based on Umbrella's threshold estimator and the red CIs are obtained with the default hard threshold method from Bio-Rad's QuantaSoft software. Since the data showed some rain, with tNOS, SPUD, and pNOS resembling Figure 1A, Umbrella consistently finds higher concentrations, because it is more robust against rain than hard thresholding methods. Our CIs are always wider as they incorporate both the uncertainty from the classification, as well as the Poisson variation. For pNOS, a deviant NTC caused high variability in the results (pNOS 1). Removing it gave stable results (pNOS 2). For pat, the rain was much heavier than for other targets, shown in Figure 1B. In pat 1, QuantaSoft software returned a "No Call" for two of the three target partition sets. In a follow-up experiment (pat 2) on a new sample, QuantaSoft did return concentration estimates.

Data and Software. The method is illustrated on data from several droplet digital PCR experiments performed on a QX100 instrument (Bio-Rad) by Biogazelle (Zwijnaarde, Belgium).

(1) A GMO detection and quantification experiment designed by Scientific Institute of Public Health (WIV-ISP), Brussels, Belgium. Species-specific and transgenic sequence templates were diluted aiming at 5000 copies/μL and 8 copies/μL based on previously obtained ddPCR data. To verify the concentration of the final dilution, the target was remeasured in all vials of the diluted samples using a single-channel ddPCR assay. At least two different vials of the diluted sample were prepared per target and three technical replicates were run on each vial. For each target, no-template controls (NTCs) were included in triplicate.

(2) A dynamic range experiment designed by Biogazelle. The cDNA input amount in the PCR was gradually increased from 5% to 45% (v/v) undiluted reverse transcription product in the final PCR and subsequently analyzed. The goal was to determine the dynamic range (and maximum input) for which the target could be properly quantified. Too much cDNA input leads to competition and inhibition of the signal. A total of nine different input amounts and an NTC were analyzed in duplicate. The data were measured on two channels and show increasing rain as a function of input amount (Figure S-6 in the Supporting Information). This dynamic range experiment can also be considered as an inhibition experiment with a variable amount of template input and inhibitor.

(3) A dedicated inhibition experiment (constant template input, variable inhibitor) designed by Biogazelle. PCR was gradually inhibited with either NEB4 restriction digest buffer (added to constant amount of digested gDNA) or RT buffer (added to constant amount of cDNA). Two experimental mixes with respective input concentrations of 40 ng of digested human gDNA (targets CLIC6 and RPP30), and 25 ng of melanoma cDNA (targets SAMMSON and RPP30) were gradually inhibited. For each mix, seven inhibition settings and an NTC were assessed in triplicate.

(4) A mutation detection experiment designed by Biogazelle. The optimal probe annealing temperature and cross reactivity is determined for four TaqMan SNP genotyping assays to be used in a mutation detection experiment. The assays are tested on digested wild-type DNA, synthetic mutant DNA, and NTC. For both DNA samples, 7200 copies were used as input.

All analyses were done in R 2.15.1 and R 3.1.2,[22] using the packages MASS (7.3−18), modeest (2.1), mgcv (1.7−29), and OrdMonReg (1.0.3). We are currently preparing an R/Bioconductor package with our method. In the meantime, all code and nonconfidential data needed to repeat the data analyses in this manuscript are available at github.com/statOmics/umbrella.

RESULTS AND DISCUSSION

Quantification. Quantification is evaluated using the GMO dataset with a high concentration stock of species-specific and transgenic sequences. In Figure 3, our concentration estimates are often higher than those obtained with the default setting of Bio-Rad's QuantaSoft software, which does not account for possible false negatives in the rain. The main Umbrella estimator (shown in blue in Figure 3) is also higher than the optional hard threshold estimator (in green). The latter conservative estimator uses a cutoff of 5% on probability to be negative and misclassified some of the rain. In experiments with light rain (tNOS and SPUD), our confidence intervals (shown in black in Figure 3) have a similar width as those from QuantaSoft (shown in red in Figure 3). In the panels on the right side of Figure 3 (pat), Umbrella gives much wider confidence intervals for the target than the QuantaSoft method.

DOI: 10.1021/acs.analchem.6b04208
Anal. Chem. 2017, 89, 4461−4467

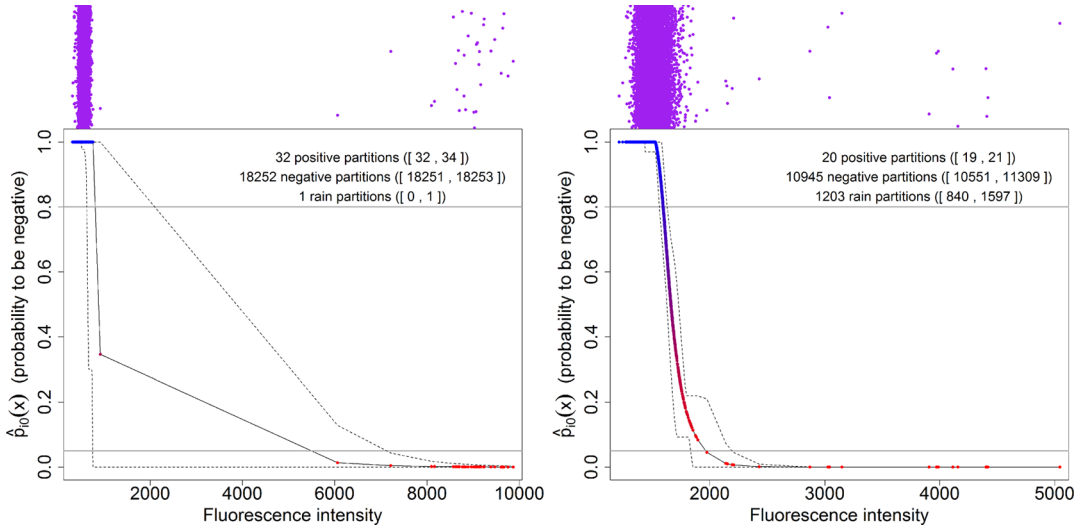

Figure 4. Partition probabilities from detection experiments. The left panel shows a partition set from the GMO experiment, while the right panel displays the results of a publicly available partition set.[8] In the left panel, the positive partitions are well-separated from the negative partitions. All partitions with a fluorescence intensity above 2000 (in red) are classified as positive ($p_{i,0,A} < 5\%$) without much doubt while only 1 partition is truly doubtful. We can confidently say that we detect target NA in the sample corresponding to the left panel and we have an estimate for its concentration. In the right panel, the positive partitions are not well-separated from the negative partitions. In all partition sets of this experiment, including the one shown here, the mixture density shows a consistent heavy tail to the right that is consistently thicker than the tails of NTC references. While a few partitions (in red) are undoubtedly positive, many more show a fluorescence intensity that is sufficiently rare, compared to the NTC reference density. Hard thresholding methods are not able to discover this pattern, while Umbrella gives the user a more-detailed view of the limitations of the experiment. Although we suspect that this sample contains target NA, we cannot draw any strong conclusions about its concentration. This type of pattern may be caused by an inhibited positive sample, a contaminated negative sample, or technical deviations as a result of baseline shifts or volume problems.

This was an experiment with heavy rain, of which one partition set is shown in the right-hand panels of Figure 1.

At the partition level, the method is more capable than the hard threshold methods, with regard to identifying and quantifying partitions in existing rain. Based on between-NTC variability, Umbrella is able to give an estimate of the probability that a partition contains no target copy, as well as a CI (Figure 2). CIs may be wide and sometimes include the complete [0;1] probability range, implying complete classification uncertainty, which is sometimes inherent to the data and appears correct. Partitions in the (far) right tail of the null density in a sample with heavy rain could realistically be all negative or positive.

The main Umbrella concentration estimator gives accurate estimates that agree with state-of-art methods on a dataset with clean data (not shown). In simulations with different settings of rain, its estimates are consistently closer to known concentrations than current standard methods (see Figure S-7 in the Supporting Information). For real data with rain, it returns concentration estimates that are less perturbed by rain and, in that sense, superior to hard thresholds. This happens because it only uses the information on the null density around its mode. Deviations in the mode estimation sometimes happen and may affect the main estimator, as shown for one of the pNOS partition sets. However, the threshold estimator is more robust to deviations in the mode estimate and is not affected. When a majority of inhibited positive partitions shows fluorescence intensities that are typical for the negative cluster, Umbrella cannot recognize them and, therefore, is unable to return accurate results. However, its bias will be smaller than that observed with current standards (see the pat example of Figure 3 and the highly inhibited examples in Figure S-7).

Detection. Concentration-based estimates can be unreliable in detection experiments, which aim for assessing the presence (absence) of a specific NA sequence in a sample. Instead, we suggest partition-specific classifiers for detection.

Umbrella returns the posterior probability $\hat{p}_{i,0,A}$ that partition i is void of NA, given its observed fluorescence intensity. It enables users to consider partitions that (a) are almost certainly positive ($\hat{p}_{i,0,A} \approx 0$), (b) may well be positive ($0 < \hat{p}_{i,0,A} < 1$, rain), and (c) are almost certainly negative ($\hat{p}_{i,0,A} \approx 1$). In our output, we provide the number of positive partitions by applying the threshold $\hat{p}_{i,0,A} < 5\%$. This alternative method gives a conservative concentration estimate, because it only counts partitions that are almost certain to be positive ($\#P$), leading to a larger estimate of the proportion of negative partitions $\hat{p}_{0,A} = 1 - \#P/n_A$. This is illustrated in Figure 4. This estimator is accurate for the data shown in the left panel, when there is no rain, but conservative for data shown in the right panel.

The number of possible rain partitions ($5\% < \hat{p}_{i,0,A} < 80\%$) is also shown in the output. In the left panel of Figure 4, the negative and positive partitions are well-separated, which translates into probabilities of either 1 (shown in blue) or 0 (shown in red), with only a single partition that may need further evaluation. In the right panel again, a few partitions are undoubtedly positive, shown in red with a probability to be negative of 0. However, the consistent heavy tail shows that many partitions have a fluorescence intensity that is so rare, relative to the NTC reference density, that they should not automatically be considered negative, resulting in probabilities not close to 0 nor 1. The CI for each partition and the number of partitions in the rain category reflect the number of doubtful partitions. Since this pattern is present in all partition sets of this experiment, it is likely that either some of the partitions were true positives or that there is a technical problem.

DOI: 10.1021/acs.analchem.6b04208
Anal. Chem. 2017, 89, 4461−4467

Umbrella thus provides the advantages of using a hard threshold when it is appropriate, while allowing for a useful measure of uncertainty when partitions cannot be easily classified. The use of a hard threshold seems appropriate for the first experiment (left panel of Figure 4), but does not take the large classification uncertainty of the second experiment (right panel of Figure 4) into account. This would lead to inaccurate results with an unrealistically small reported precision.

Quality Control. When the null density has heavy tails (for example, due to nonconstant partition volumes or baseline shifts), Umbrella will correct for this if NTCs show the same pattern. It will provide realistic estimates, possibly with wide confidence intervals for partitions in the tails (e.g., the right panel of Figure 4). Relatively small deviations between partition sets may have a substantial impact on the partition estimates in the tail. The CIs at the partition level are a unique tool to understand the true variability of their potential classification.

The width of a partition-specific CI can be used as a quality measure to identify partitions or partition sets with deviating properties, for example, because of volume problems or changes in baseline fluorescence correction within or between partition sets. Both instances are reflected in skewed densities with long tails, which can be recognized by wide confidence intervals around the right tail of the negative cluster. An example is shown in the Supporting Information.

Sometimes, the CI of the overall robust estimator may also indicate quality issues. In the pNOS example of Figure 3, the first of the three NTCs showed a substantially deviating pattern from the others. This is immediately reflected in the very wide confidence intervals shown under "pNOS 1". When this deviant NTC was dropped when estimating the null component, the problem was resolved and CIs with natural widths are recovered under "pNOS 2". The automatic method of Bio-Rad did not discover this problem and it is also difficult to pick it up by eye, even after being aware of the problem (see the Supporting Information).

Multichannel Data. Our model-based clustering method can also be used for obtaining concentration estimates from multichannel data. Upon suitable preprocessing, it can be adopted on univariate projections. The procedure is illustrated on the two-channel dynamic range, inhibition, and validation of mutation detection datasets.

The dynamic range dataset showed a substantial tilt (Figure S-6). Our fully automated procedure was able to correct for rotation and cross-talk while obtaining plausible concentration estimates. The results were consistent with those from Bio-Rad's QuantaSoft software when using a manual, subjective threshold where the cutoff was placed as closely to the negative cluster as possible. This highly subjective and researcher-dependent threshold was only possible because we had prior information on the experiment. The automated threshold of the QuantaSoft software produced inferior results, because it classified many partitions in the rain as negative. Umbrella is objective, recognizes rain, and assigns realistic probabilities to its partitions. The basic concentration estimator $\hat{p}_0$ showed relatively high variability between the technical duplicates. In contrast, taking the average of the partition probabilities as the concentration estimator showed similar between-duplicate variability as the results from the QuantaSoft software while retaining other advantages. This estimator may show potential for multichannel data.

In the dynamic range dataset, digital PCR is able to quantify the concentration correctly for up to 20% (v/v) cDNA input. With a subjective manual threshold and the model-based clustering method, 25% (v/v) could be achieved in one channel and 30% (v/v) in the other. In addition, Umbrella is able to detect targets up to 40% (v/v), a setting in which the standard methods return either a "No Call" or "no target detected" (Figure S-12 in the Supporting Information).

In the mutation detection experiment, some partition sets showed clear nonspecific amplification. This caused rotational issues in single false positive clusters appearing as "upward rain" in one-dimensional QuantaSoft plots (Figure S-8 in the Supporting Information). Umbrella corrects for rotation and also recognized a higher variation in single positive clusters, which were, on average, about a third wider than the null reference. As a result, we obtained remarkably fewer false positives, compared to hard thresholding in the QuantaSoft software (Supporting Information, Section 10) while giving similar concentration estimates as the reference on the concordant channel (Figure S-11 in the Supporting Information).

The quality control provided by our method can help researchers understand when the results are not an indication of a clean sample without target, but rather of a problematic sample that requires revision. In the inhibition experiments, for instance, Umbrella was able to objectively match the result of the default hard thresholding provided by Bio-Rad's QuantaSoft software when the amount of buffer was limited. While it was impossible to find target when there was too much buffer for any method, our method did find that the density of seemingly negative (highly inhibited) partition sets was atypical and different from the expected density of NTCs. We noticed that the density of highly inhibited sets showed less variation and had a higher peak, which was clearly visible when the ratio with the null (NTC) density was taken. This property was not visible by eye but could be used as quality control in experiments. More details and other methods for QC can be found in the Supporting Information.

CONCLUSIONS

Many sources of variation affect the precision of dPCR concentration estimates.[23] Most contributions treat the inherent Poisson variation embedded in each technical run as the primary source of variation, while other sources of variation within or between partition sets are largely ignored. The classification uncertainty, for instance, has been identified as a major source of variation within partition sets.[6]

While manufacturers and users alike may prefer hard thresholds for simplicity, we feel that it is important to acknowledge that the outcome of every partition is subject to random variability. Umbrella quantifies the precision of the classification for each partition by reporting the probability that it belongs to a specific cluster. The quantification of this precision is, itself, a first step that captures a single additional variance component and, thus, subject to further improvement. Nevertheless, it is important to acknowledge classification variation to avoid reporting unrealistic precision. Ideally, this approach is extended to include additional variance components, within and between partition sets and technical repeats, such as unequal partition volumes and sampling errors.

The partition-specific probabilities are useful quality measures, which can flag problematic partitions that are difficult to quantify. The method is able to address heavy tails in the

DOI: 10.1021/acs.analchem.6b04208
Anal. Chem. 2017, 89, 4461−4467

intensity distribution of negative partitions, which appear as a consequence of unequal volumes or baseline changes. With substantial rain, Umbrella acknowledges the classification uncertainty of partitions in the right tail of the null density. Unfortunately, this is also occasionally reported to be due to the technical and stochastic variation of the observed null density between partition sets, which is a feature that may yet turn out to be avoidable.

When results are reported, the final judgment resides with the critical user. Blindly applying hard thresholds risks the cultivation of a false sense of security and an overt trust in the technology. Additional software support may routinely provide the info needed (including a wide range of quality control measures) to optimize performance of the technology.

■ ASSOCIATED CONTENT

Supporting Information

The Supporting Information is available free of charge on the ACS Publications website at DOI: 10.1021/acs.analchem.6b04208.

Detailed information on mixture models for dPCR quantification, in-depth description of the data, Supporting Figure S1−S15 and Supporting Table S1−S6 (PDF)

■ AUTHOR INFORMATION

Corresponding Authors

*Tel.: +3292644756. E-mail: bartkm.jacobs@ugent.be (B. K. M. Jacobs).

*Tel.: +3292644904. E-mail: lieven.clement@ugent.be (L. Clement).

ORCID

Bart K. M. Jacobs: 0000-0002-4677-0911

Author Contributions

B.J., L.C., and E.G. conceived the study, developed the model and wrote the manuscript. B.J. and L.C. wrote the software implementation. J.V., A.B., A.D., N.N., N.R., and N.P. performed the dPCR experiments and provided the data. B.J. conducted the case study. J.V., N.R., and N.P. contributed to the interpretation of the dPCR results, the discussion, and the conclusions.

Notes

The authors declare no competing financial interest.

■ ACKNOWLEDGMENTS

Part of this research was supported by IAP research network "StUDyS" Grant No. P7/06 of the Belgian government (Belgian Science Policy) and Multidisciplinary Research Partnership "Bioinformatics: from nucleotides to networks" of Ghent University. The authors would like to thank the anonymous referee for bringing the additional application of nonspecific amplification in mutant detection to our attention.

■ REFERENCES

(1) Köppel, R.; Bucher, T. *Eur. Food Res. Technol.* **2015**, *241*, 427−439.

(2) Dobnik, D.; Spilsberg, B.; Bogožalec Košir, A.; Holst-Jensen, A.; Žel, J. *Anal. Chem.* **2015**, *87*, 8218−8226.

(3) Sedlak, R. H.; Jerome, K. R. *Diagn. Microbiol. Infect. Dis.* **2013**, *75*, 1−4.

(4) Strain, M. C.; Lada, S. M.; Luong, T.; Rought, S. E.; Gianella, S.; Terry, V. H.; Spina, C. A.; Woelk, C. H.; Richman, D. D. *PLoS One* **2013**, *8*, e55943.

(5) Whale, A. S.; Huggett, J. F.; Cowen, S.; Speirs, V.; Shaw, J.; Ellison, S.; Foy, C. A.; Scott, D. J. *Nucleic Acids Res.* **2012**, *40*, e82−e82.

(6) Jacobs, B. K.; Goetghebeur, E.; Clement, L. *BMC Bioinf.* **2014**, *15*, 283.

(7) Dreo, T.; Pirc, M.; Ramšak, Ž.; Pavšič, J.; Milavec, M.; Žel, J.; Gruden, K. *Anal. Bioanal. Chem.* **2014**, *406*, 6513−6528.

(8) Trypsteen, W.; Vynck, M.; De Neve, J.; Bonczkowski, P.; Kiselinova, M.; Malatinkova, E.; Vervisch, K.; Thas, O.; Vandekerckhove, L.; De Spiegelaere, W. *Anal. Bioanal. Chem.* **2015**, *407*, 5827−5834.

(9) Jones, M.; Williams, J.; Gärtner, K.; Phillips, R.; Hurst, J.; Frater, J. *J. Virol. Methods* **2014**, *202*, 46−53.

(10) Huggett, J. F.; Cowen, S.; Foy, C. A. *Clin. Chem.* **2015**, *61*, 79−88.

(11) Madej, R. M.; Davis, J.; Holden, M. J.; Kwang, S.; Labourier, E.; Schneider, G. J. *J. Mol. Diagn.* **2010**, *12*, 133−143.

(12) European Network of GMO Laboratories (ENGL). *Definition of Minimum Performance Requirements for Analytical Methods of GMO Testing*, 2015.

(13) Weighardt, F. *Nat. Biotechnol.* **2007**, *25*, 1213−1214.

(14) Milavec, M.; Dobnik, D.; Yang, L.; Zhang, D.; Gruden, K.; Žel, J. *Anal. Bioanal. Chem.* **2014**, *406*, 6485−6497.

(15) Fraley, C.; Raftery, A. E. *J. Am. Stat. Assoc.* **2002**, *97*, 611−631.

(16) Kask, P.; Palo, K.; Ullmann, D.; Gall, K. *Proc. Natl. Acad. Sci. U. S. A.* **1999**, *96*, 13756−13761.

(17) Schwartz, J. A.; Vykoukal, J. V.; Gascoyne, P. R. *Lab Chip* **2004**, *4*, 11−17.

(18) Corbisier, P.; Pinheiro, L.; Mazoua, S.; Kortekaas, A.-M.; Chung, P. Y. J.; Gerganova, T.; Roebben, G.; Emons, H.; Emslie, K. *Anal. Bioanal. Chem.* **2015**, *407*, 1831−1840.

(19) Kask, P.; Palo, K.; Fay, N.; Brand, L.; Mets, Ü.; Ullmann, D.; Jungmann, J.; Pschorr, J.; Gall, K. *Biophys. J.* **2000**, *78*, 1703−1713.

(20) Efron, B.; Tibshirani, R. *Ann. Stat.* **1996**, *24*, 2431−2461.

(21) Huggett, J. F.; Foy, C. A.; Benes, V.; Emslie, K.; Garson, J. A.; Haynes, R.; Hellemans, J.; Kubista, M.; Mueller, R. D.; Nolan, T.; Pfaffl, M. W.; Shipley, G. L.; Vandesompele, J.; Wittwer, C. T.; Bustin, S. A. *Clin. Chem.* **2013**, *59*, 892−902.

(22) R Core Team. *R: A Language and Environment for Statistical Computing*; R Foundation for Statistical Computing: Vienna, Austria, 2012; ISBN 3-900051-07-0.

(23) Pinheiro, L. B.; Coleman, V. A.; Hindson, C. M.; Herrmann, J.; Hindson, B. J.; Bhat, S.; Emslie, K. R. *Anal. Chem.* **2012**, *84*, 1003−1011.

DOI: 10.1021/acs.analchem.6b04208
Anal. Chem. 2017, 89, 4461−4467